

Tina Memo No. 2004-002
Short version presented at MIUA 2005

Trends in Brain Volume Change with Normal Ageing

P. A. Bromiley, N.A. Thacker, M. Jones, N. Purandare, A. Varma and A.
Jackson

Last updated
16 / 3 / 2006



Imaging Science and Biomedical Engineering Division,
Medical School, University of Manchester,
Stopford Building, Oxford Road,
Manchester, M13 9PT.

Trends in Brain Volume Change with Normal Ageing

P. A. Bromiley, N. A. Thacker, M. Jones, N. Purandare, A. Varma and A. Jackson,
Imaging Science and Biomedical Engineering Division,
Medical School, University of Manchester,
Stopford Building, Oxford Road,
Manchester, M13 9PT.
`paul.bromiley@man.ac.uk`

Abstract

In order to measure cerebral atrophy due to neurodegenerative diseases, the major confounding factor of normal age-related atrophy must be taken into account. Furthermore, in order to compare cerebral volume measurements across multiple subjects, normalisation for differences in head size is also required. We describe an investigation of these normalisations based on measurements of cerebro-spinal fluid (CSF) volumes in MR images of 70 normal volunteers. First, we demonstrate that, to within the limits imposed by segmentation errors, normalisation to the total intracranial volume (TIV) (the usual normalisation for head size differences) is statistically identical to normalisation to the volume of the bounding box of the CSF space, a quantity that is considerably easier to compute. Second, we investigate several possible functional dependencies for CSF volumes with age, and conclude, based on a combination of goodness-of-fit probabilities and biological plausibility, that the dependence obeys a Weibull cumulative distribution function. We also investigate the regional dependency of CSF volumes with age at coarse scales, and conclude that CSF volume increase due to normal ageing occurs uniformly throughout the cranium. Finally, we describe a meta-study in which our results are compared to previously published CSF and TIV measurements. This study incorporates measurements from ≈ 1300 subjects, and shows close agreement between the separate studies involved.

1 Introduction

Dementia affects over 25 million people worldwide, with over 750,000 sufferers in the United Kingdom alone (see www.alzheimers.org.uk). Symptomatic treatments that slow cognitive decline, cholinesterase inhibitors and memantine, are currently available for Alzheimer's disease (AD), the most common cause of dementia. There is also increasing recognition of the overlap between AD and cerebrovascular disease with prospects for prevention of both AD and vascular dementia (for review, see [32]). This highlights the importance of early diagnosis of dementia, its type, and identification of people 'at risk' of developing dementia. In this respect, structural neuroimaging, to measure volume loss of medial temporal lobe, hippocampus, or entorhinal cortex, may be particularly important in identifying patients with 'mild cognitive impairment' [33, 15], especially those who will go on to develop dementia, especially AD [29]. However, hippocampal atrophy can also be seen in vascular dementia [2] and fronto-temporal dementia [23]. The techniques used to measure regional atrophy vary considerably, with no evidence of added diagnostic value for most techniques [22]. Also, estimating volumes of individual structures on neuroimaging is expensive and time consuming with considerable inter-rater and inter-individual variations limiting use in clinical practice [30]. In the clinical setting, the neuroimaging report (in the UK, often CT) may vary from 'normal or no atrophy', 'involutional changes or atrophy appropriate for age', to 'mild to moderate atrophy'. These decisions are subjective and reliant on the experience of the rater. There is a need to develop a technique, which is simple, automated, and accurate in deciding whether the observed volume of the brain or atrophy is more than that expected from age and gender alone.

Distinctive patterns of accelerated cerebral atrophy are a feature of a large number of neurodegenerative and dementing disorders such as Alzheimer's disease, frontotemporal dementia, Parkinson's disease and others. The feasibility of using relatively coarse regional measurements of brain volume to diagnose the above diseases has been demonstrated previously [42]. However, in order to achieve maximum diagnostic utility, such techniques must also take into account the expected amount of normal age-related atrophy for any given age. Brain volume loss is thought to be an inevitable consequence of normal human ageing [20]. A number of studies have set out to define these changes, but no consensus has been reached. There are marked methodological differences between studies including those that are longitudinal [37, 16], those that are cross sectional [3, 25, 13, 31, 12, 24], and those employing both of these methods [39]. There remains dispute as to whether the atrophy that occurs in normal ageing follows a linear or non-linear course. In vivo quantification of total and regional brain atrophy is being developed as a means of diagnosing many neurodegenerative conditions, which as the population gets older as

a whole, are certain to become more prevalent. In addition to diagnosis, the need to monitor treatment effects for new therapies in these diseases is likely to become important. For both of these purposes it is necessary to understand what constitutes normal ageing of the human brain, and specifically what degree of brain atrophy can be expected on neuroimaging as a consequence of normal ageing. The changes seen in subjects suspected of having, or being at risk of, neurodegenerative diseases can then be corrected for this confounding variable. The purpose of the work described here was to determine these correction factors for age-related atrophy for arbitrary coarse ($\approx 10 - 100\text{cm}^3$) regions of the brain.

Previous work on the effects of normal ageing on brain volume [3] [7] [9] [8] [12] [13] [44] [25] [31] has focused on measurements of grey and/or white matter volumes. We instead measured only cerebro-spinal fluid (CSF) volumes. Since the interior volume of the cranium is approximately fixed throughout adulthood [13], increases in CSF volume provide an accurate marker for decreases in grey and white matter volume. The drawback of measuring CSF is that volume changes cannot be ascribed to specific tissue locations. However, since the CSF is a liquid, the variation in physical properties between the CSF and the other tissues present in the cranium, which are solids, is greater than the variation in physical properties amongst the other tissues. It is therefore possible to design MR pulse sequences that result in greater mean grey-level separation between CSF and other tissues than can be obtained for any other pair of tissues. The signal-to-noise ratio for CSF segmentation is therefore higher than for any other tissue, and the segmentation is consequently more accurate. In addition, since the errors on the volume measurements presented here were observed to be Poisson-like, and the CSF volume is much lower than the combined grey and white matter volume ($\approx 7 - 9\%$ of the total intra-cranial volume between early childhood and adolescence [13]), any trends in the volume change are much more apparent. This allows such trends to be identified more accurately, and therefore allows some conclusions on the underlying biological processes that lead to age-related atrophy to be drawn.

2 Materials and Methods

2.1 Volunteers

Study participants included 70 healthy controls (32 male and 38 female) ranging in age from 19 to 85 years with a mean age of 57 ± 20 years. All subjects underwent cognitive assessment including the Mini-Mental State Examination (MMSE) to exclude significant cognitive impairment suggestive of undiagnosed dementia [17], and none had vascular risk factors. The local ethics committee approved the research, and informed consent was given for inclusion in the study by the subjects.

2.2 Imaging

All subjects underwent MR imaging with a 1.5-T system (ACS-NT, with PowerTrack 6000 gradient subsystem; Phillips Medical Systems, Hamburg, Germany) with a birdcage head coil receiver. Fast spin-echo inversion-recovery images (repetition time, 6850 msec; echo time, 18 msec; inversion time, 300msec; echo train length, 9) were obtained in contiguous 3-mm thick sections throughout the brain, with an in-plane resolution of 0.89mm^2 (matrix, 256×204 , field of view, $230 \times 184\text{mm}$), and real image reconstruction was performed. Figure 1 shows a typical example of the data. The youngest twelve patients, ranging in age from 19 to 53 years with a mean age of 35 years, were scanned multiple times, with two sets of image volumes being acquired an hour apart. A further two sets of images volumes, again acquired an hour apart, were obtained from eight of these patients a year later. These multiple image volumes were then used in repeatability studies, to determine the relative magnitudes of analysis errors and the inherent biological variability of the volume measurements.

2.3 Image Analysis

Analysis of the image data was performed using the TINA medical image analysis software (www.tina-vision.net) and consisted of three stages. First, all MR volumes were coregistered to the volume that represented the median of the patient group in terms of its atrophy pattern, using rigid Mutual Information based coregistration [4, 5], allowing subsequent analysis of the results in a standard coordinate system. Second, the CSF was segmented using a technique based on fitting a partial volume model of the tissues present in the head to the histogram of the image volumes [35, 34, 41]. In order to reduce the processor time required, two cuboidal regions were defined in the standard coordinate system, lying within the skull and covering the anterior and posterior six slices containing the ventricles. The combined region contained only grey matter, white matter and CSF, and could therefore be

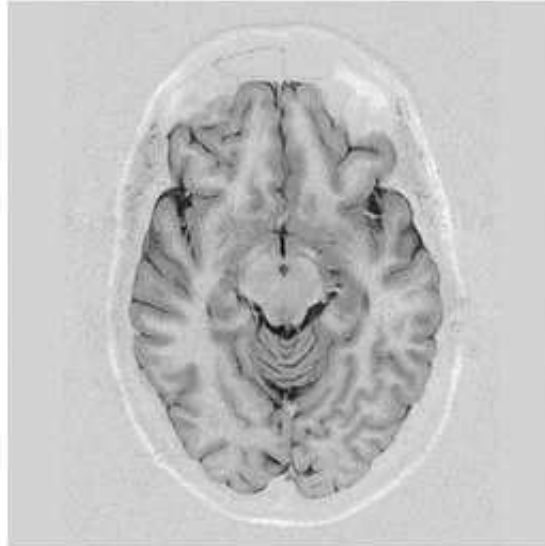


Figure 1: Typical slice from a fast spin-echo inversion recovery MR image volume.

described using a model consisting of only three tissues, comprising Gaussian components to represent the pure tissues, and triangular distributions convolved with Gaussians to represent the partial volume contributions for all three pairs of tissues. Each component was described by three parameters: a mean grey level, a standard deviation, and a prior term representing the probability of occurrence of the component, giving a total of eighteen parameters. The model was fitted to the histogram of the image volumes using the Expectation-Maximisation algorithm. Volumetric maps of the CSF distribution were then produced from the models, and binarised at the 0.5 probability threshold to produce a CSF segmentation. The segmented images were then multiplied with a set of binary masks produced in the standard coordinate system. The masking had two purposes: to delete non-CSF fluid spaces (e.g. eyes, sinuses) and to enforce a consistent inferior boundary to the measurement space, defined by drawing a line in the mid-sagittal section parallel to the horizontal axis that passed through the junction of the calvarium and the tentorium cerebelli. The anterior, posterior, lateral, and superior boundaries of the CSF space were automatically identified by locating the extremes of the CSF. Finally, the number of voxels in the binarised, masked CSF maps was counted and multiplied by the voxel size to produce a measurement of the CSF volume. Figure 2 shows a typical CSF segmentation.

In order to avoid errors in the CSF volume measurements due to interpolation, all CSF measurements were performed in the original coordinate system of the data, and the coregistration was used only to align the masks. Therefore, normalisation for head size differences was also required. This was performed through division of all volume measurements by total intra-cranial volume (TIV), which been shown [44] to be an effective normalisation for both inter-individual variations in head size and variation in voxel sizes in longitudinal studies. The main effect of this normalisation was to correct for sex-linked differences in head size, which was found (consistent with previous studies e.g. [13], [44]) to be on average 8% lower in females than in males. TIV measurements were produced using a semi-independent segmentation technique, in order to allow comparisons of the TIV to the volume of the bounding box on the CSF. This segmentation technique involved binary thresholding at a level determined through fitting a six-tissue partial volume model, with components for bone, fat, air, white matter, grey matter and CSF, to the histogram of the MR image volumes using the simplex algorithm [36].

2.4 Statistical Analyses of Volume Measurement Data

Once the TIV normalised CSF volume measurements had been produced, the functional dependency of the CSF volumes with age was investigated. Two types of process could be envisaged¹. The first would be a mechanism resulting in continuous volume loss, such as might be seen in dehydration or demyelination that occurs in diseases such as alcoholism and multiple sclerosis. The second would be a volume loss associated with the loss of discrete units (e.g. neurons). A continuous process would result in a polynomial dependency, with the observed trend

¹We assume that, as is generally accepted, the increase in CSF volume with age is due to the loss of grey and/or white matter, rather than any process inherent to the CSF itself (such as an increase in CSF pressure).

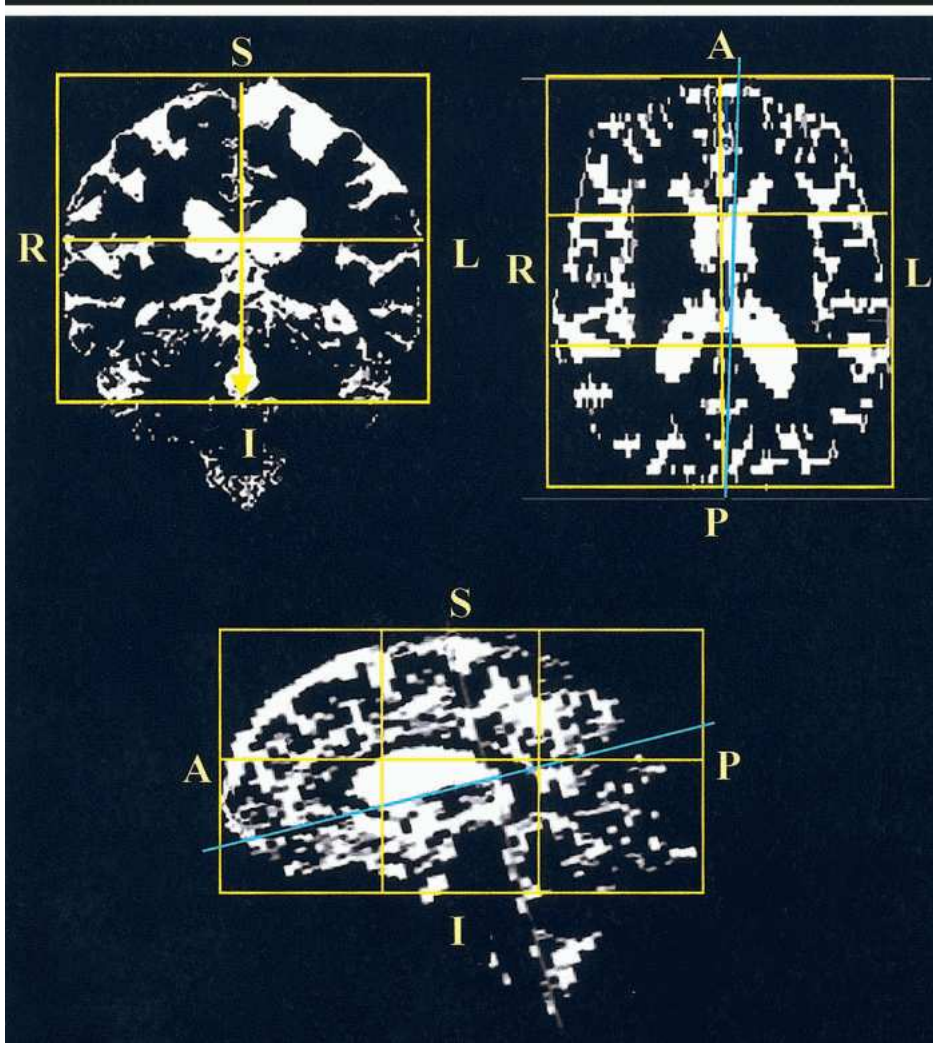


Figure 2: Typical binarised CSF segmentation.

in CSF volume being the cumulative distribution function (i.e. integral with respect to time) of the probability distribution function describing the loss process. A continuous process with a constant rate of volume loss would result in a linear dependence of CSF volume with age: a bi-linear function was used to represent this possibility, allowing for a non-zero age of onset for the atrophy (set to 55 years, identified in [13] as the age of onset of accelerated volume loss). A quadratic function was used to represent a continuous process with a linearly increasing rate of volume loss. If the atrophy were due to the loss of discrete units with a constant probability, i.e. a Poisson process, then an exponential decrease in brain volume would be observed. Finally, systems that exhibit loss of discrete units with a time-dependent probability usually exhibit a Weibull distribution i.e. a Poisson process with a power-law dependency for the probability of unit loss with time. This function [43], is commonly observed in systems where the decay of a given unit increases the probability of decay in those remaining, and is the most widely used distribution in reliability analysis. Given the high level of interconnectivity present in the brain, we hypothesise that this is a biologically plausible function to describe age-related atrophy. Each of these functions was fitted to the data, and the goodness-of-fit probabilities were compared.

In addition, the regional distribution of CSF volume increase with age was investigated at coarse ($\approx 10 - 100\text{cm}^3$) scales. We adopted the same approach used in our previous work [42] to investigate the regional dependence of CSF volume change on disease. The intracranial volume was divided into twelve equi-sized volumes, using planes to divide the CSF space into anterior, middle, and posterior thirds, superior and inferior halves, and lateral halves, as shown in Fig.2. The functional dependency of CSF volume on age in each of these regions, and in combinations of contiguous regions, was investigated in order to highlight any regional differences. This procedure allowed investigation of such regional differences independent of any hypothesised behaviour (e.g. dividing the brain into lobes).

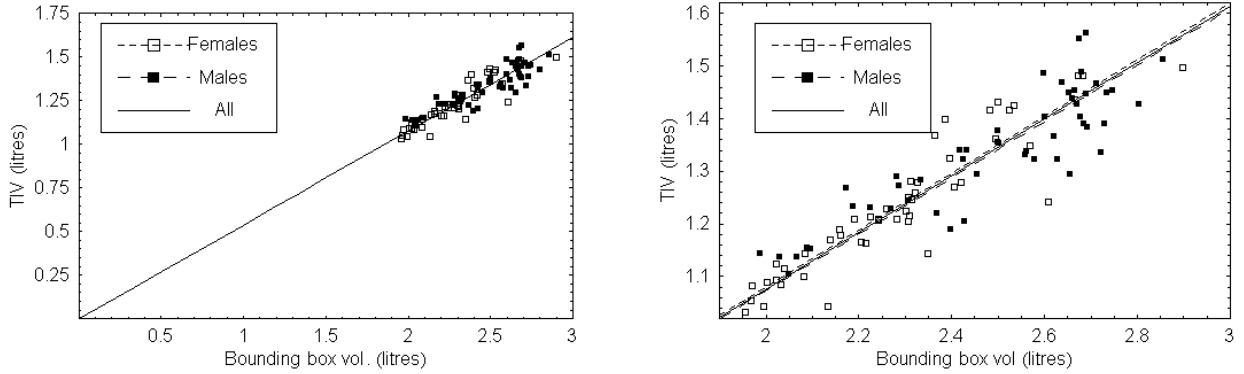


Figure 3: The relationship between the TIV and the CSF bounding box size for head-size normalisation. Linear fits are shown for all data and for males and females separately.

Finally, a literature survey was conducted to collect previously published measurements of TIV and CSF volumes from MR images. These measurements were used to conduct a meta-study, incorporating data from ≈ 1300 individuals. The study was designed to cover multiple MR sequences, definitions of the measurement space (i.e. definition of the lower bound on the CSF volume), and segmentation algorithms, in order to demonstrate the maximum variation in TIV normalised CSF volume measurements that can be produced through variations in the experimental procedure. The previous measurements were then compared to the data presented here, in order to confirm the accuracy of our segmentation process.

3 Results

3.1 Head Size Normalisation

In order to allow direct comparisons of cerebral volumes across multiple subjects, variations in head size must be taken into account. This is usually performed through normalisation to the total intracranial volume (TIV), which has been shown [44] to be an effective normalisation for both inter-individual variations in head size and variation in voxel sizes in longitudinal studies. In previous work [42] we have used a simpler alternative, finding the product of the maximal CSF extents in the anterior-posterior, lateral, and superior-inferior directions, multiplying these to produce the volume of a bounding box on the CSF space, and dividing all volume measurements by this volume in order to normalise for head size. CSF segmentation can be performed more accurately than segmentation of the other tissues present in the cranium, as described above, and so normalisation to the CSF bounding box volume is potentially simpler than normalisation to the TIV. In order to compare the two normalisations, measurements of CSF bounding box volume and TIV were obtained through semi-independent segmentation techniques, as described above. Figure 3 shows TIV plotted against CSF bounding box volume, together with linear fits to the data for males and females separately, and for males and females combined.

Sex	TIV (mean \pm s.d.)	Bounding box volume (mean \pm s.d.)	Linear fit
Males	1.338 ± 0.116	2.490 ± 0.231	$TIV = 0.536 \text{ bound}$
Females	1.234 ± 0.127	2.285 ± 0.214	$TIV = 0.540 \text{ bound}$
All	1.288 ± 0.132	2.392 ± 0.245	$TIV = 0.538 \text{ bound}$

Table 1: Comparisons of TIV to the volume of the bounding box on the CSF space. All volumes are quoted in litres.

The bounding box volumes and TIV are directly proportional, and the ratio of the standard deviation to the mean of the measurements is approximately the same (10.2% in both cases), showing that CSF bounding box and TIV normalisations are statistically equivalent to within the limits imposed by segmentation errors. In addition, there is no statistically significant difference between the regression lines for males, females, and both groups combined.

Table 1 gives the mean bounding box volumes, TIVs and linear fits to the data for males, females, and both groups combined. Due to the definition of the measurement space used here, the TIV measurement is an underestimate

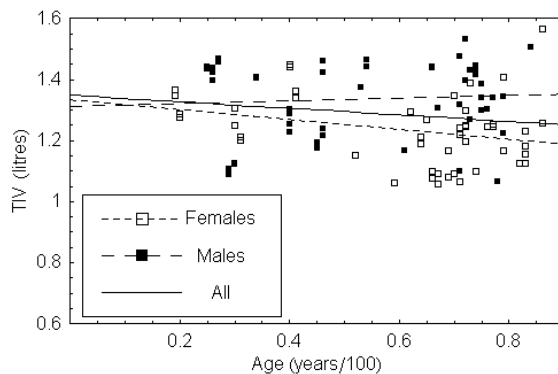


Figure 4: The relationship between the TIV and age for males, females, and both groups combined: linear fits to the data are shown.

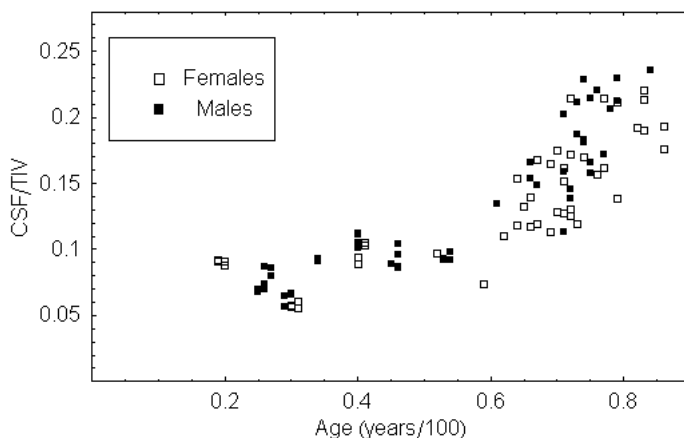


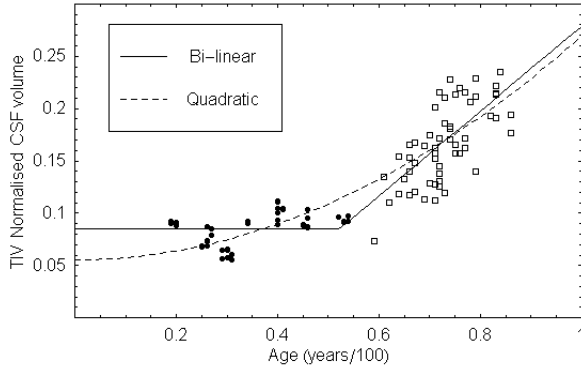
Figure 5: TIV normalised CSF volumes for both male and female subjects

of true TIV. However, the measurements agree to within errors with previous work in which similar definitions of the measurement space have been used (e.g. [26, 31, 12]).

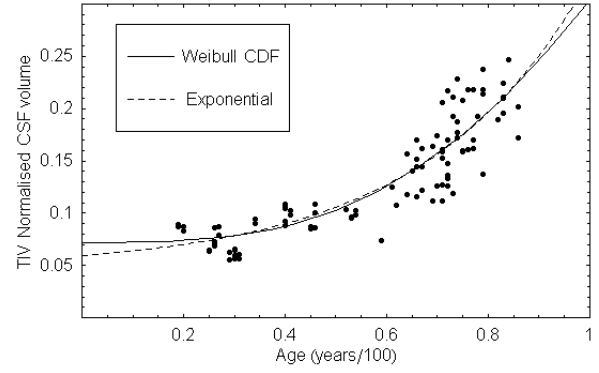
Figure 4 shows the dependence of TIV on age. It is possible to hypothesise that differences in maternal or childhood nutritional status over the last century could result in a negative correlation between TIV and age, and indeed some authors have reported finding such a correlation e.g. [25] found a significant negative correlation for males but not for females. However, most authors (e.g. [31, 3, 44, 12, 13, 27]) report no significant correlation, and none was found in the data presented here at the 95% confidence limit ($P=0.61$ for males, 0.098 for females, and 0.053 for both groups combined).

3.2 Age Dependency of CSF Volume

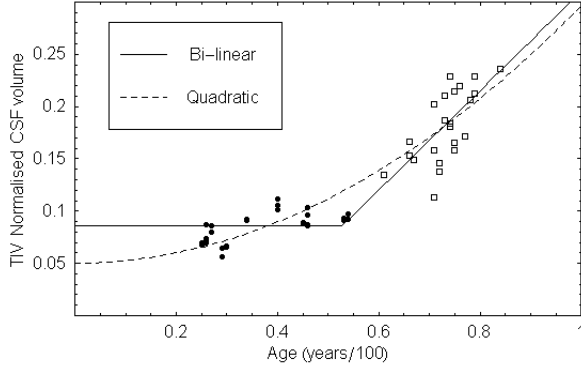
Figure 5 shows the distribution of normalised total CSF volumes with age. A markedly non-linear trend can be seen in the data. Previous studies have produced some evidence for such a trend: for example, [13] observed elevated rates of atrophy in older subjects, but not at statistically significant levels, whilst [39] observed significantly increasing rates of atrophy with age. The presence of a significant non-linear trend in the data presented here allows speculation on the biological mechanism underlying age-related atrophy. As described above, two types of process could be envisaged: a continuous process, which would lead to a polynomial dependence of CSF volume on age, or a process due to the loss of discrete units i.e. a Poisson-type process. In order to investigate these hypotheses, several candidate functions were fitted to the data. Bi-linear and quadratic functions were used to represent continuous processes with constant and linearly increasing rates of volume loss respectively, and exponential and Weibull CDF functions were used to represent Poisson-type processes with constant and power-law dependent probabilities of unit loss with time respectively. The non-polynomial functions were fitted using the Levenberg-Marquadt technique. Since the data represent the result of a counting process they were subject to Poisson errors,



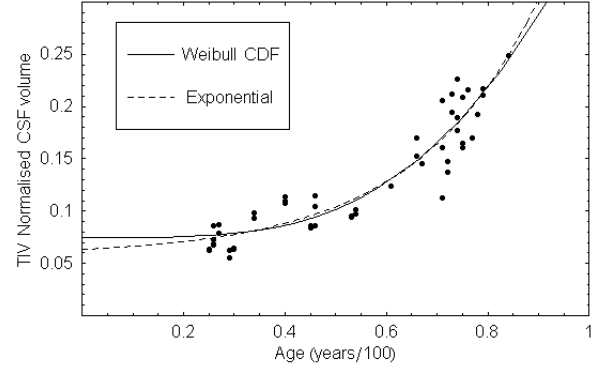
(a) All subjects: polynomial functions.



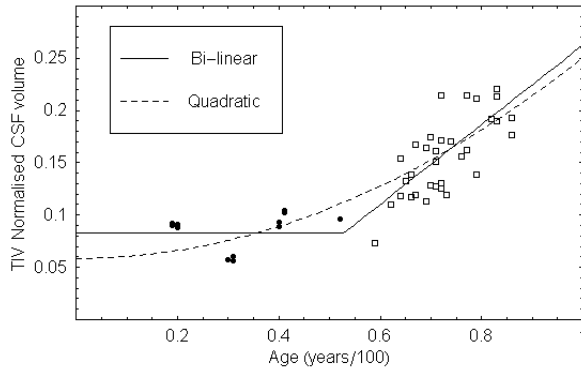
(b) All subjects: Poisson-type functions.



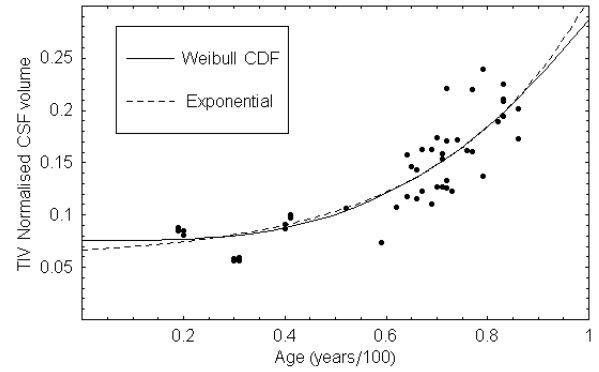
(c) Male subjects: polynomial functions



(d) Male subjects: Poisson-type functions



(e) Female subjects: polynomial functions



(f) Female subjects: Poisson-type functions

Figure 6: Bi-linear, quadratic, exponential and Weibull CDF fits to the TIV normalised CSF volumes for male (c, d), female (e, f), and all (a, b) subjects. In graphs a, c, and e, the difference in the plot symbols shows the splitting of the data at the age of senescence for the bi-linear fit.

and so were weighted by their square-root during the fitting process in order to normalise their variances [40]. Figure 6, show the fitted functions for males, females, and both groups combined.

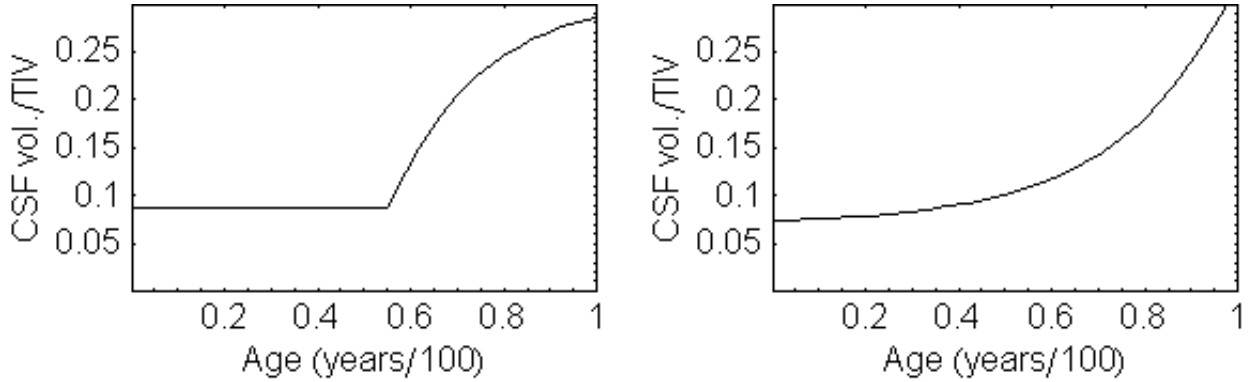


Figure 7: Trends in TIV normalised CSF volume expected from an exponential decrease in total parenchymal volume with a specific age of onset (a) and an exponential increase in CSF volume (b). Scenario (b) more accurately reflects the trend observed in the data.

Name	Function	Fit probability (males) (%)	Fit probability (females) (%)	Fit probability (all) (%)
Bi-linear	$y = a \quad (x < 0.55)$ $y = bx + c \quad (x > 0.55)$	35.0	81.4	2.95
Quadratic	$y = ax^2 + b$	37.5	56.2	49.0
Exponential	$y = a + be^{cx}$	94.1	86.4	85.9
Weibull CDF	$y = a - (1-a)(1 - e^{-(x/b)^c})$	100.0	100.0	100.0

Table 2: Errors on functions fitted to the total normalised CSF volumes measurements shown in Figure 6. All fit probabilities are relative to the Weibull CDF fit.

No independent estimate of the errors was available and so χ^2 goodness-of-fit probabilities could not be calculated in the usual way. Instead a noise estimate was obtained from the Weibull CDF fit, which had the lowest residuals, assuming a χ^2 per degree of freedom of one, and used to calculate relative goodness-of-fit probabilities for the other functions. These are given in Table 2. Given that there is no indication that any of the hypothesised fit functions is over-fitting the data, this procedure can only underestimate the χ^2 of the Weibull CDF fit, and so all of the goodness-of-fit probabilities must be scaled by a constant larger than unity relative to those that would be obtained from an accurate estimate of the errors. Therefore, any conclusions based on these probabilities (in terms of rejecting any of the fits) will be conservative.

The data available for female subjects below the age of 50 was sparse, and so lacked the statistical power to reject any of the fit functions. However, combining the probabilities for the separate fits to males and females gives a value of 21.1% for the quadratic function and 28.5% for the bi-linear function. Whilst these are not sufficient for categorical rejections of either function, bearing in mind that they are conservative estimates of the true goodness-of-fit probabilities, they are sufficient to show that the polynomial functions provide significantly worse explanations of the data than the Poisson-type functions. Further evidence for this conclusion is provided by the low probability for the bi-linear fit to the entire data set, which allows the function to be rejected at the 95% confidence level.

The exponential and Weibull CDF functions have statistically equivalent goodness-of-fit probabilities. However, the exponential function can be rejected on the grounds of biological plausibility. The data show an increasing rate of CSF volume growth with time: the exponential fit therefore represents an exponentially increasing CSF volume. However, since the measurements have been normalised to the TIV, the CSF volume is the complement of the total parenchymal volume, not its inverse. An exponential decrease in total parenchymal volume would produce the opposite trend in CSF volume: Fig.7 shows the two alternatives. Since the process leading to age-related atrophy is presumably inherent to the grey and/or white matter, we must conclude that an exponential increase in CSF volume, which would have to be due to a process such as increasing intra-cranial pressure, cannot be a biologically plausible mechanism, and reject the exponential fit. Therefore, we tentatively conclude that the process underlying age-related cerebral atrophy exhibits a Weibull CDF dependence on age. This indicates that age-related atrophy is due to a loss of discrete units of tissue from within the brain, with a probability of unit loss that increases with time. This functional dependence is commonly exhibited by systems in which the decay of a given unit increases

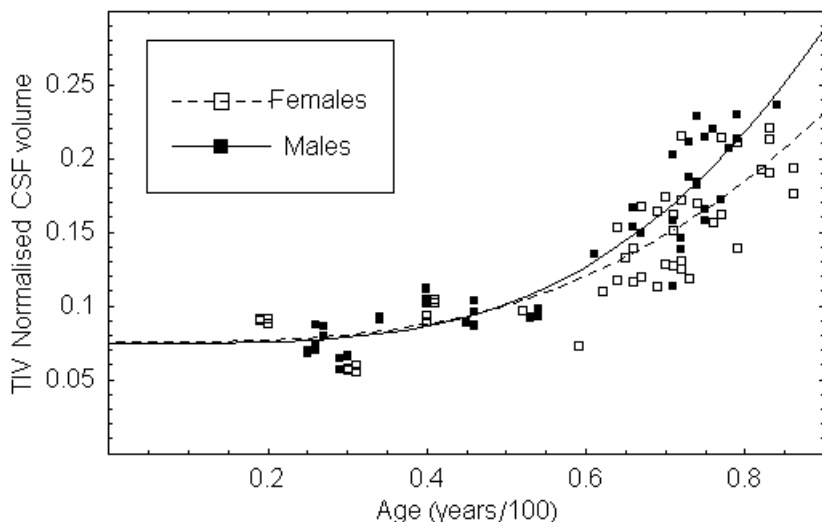


Figure 8: Weibull CDF fits to TIV normalised CSF volumes for male and female subjects.

the probability of decay in the units around it. Since the brain is a highly interlinked system, we conclude that this is a biologically plausible mechanism for age related atrophy.

Figure 8 shows the Weibull CDF fits to male and female subjects. Male subjects exhibited a significantly faster rate of atrophy than females ($P=0.026$), as found in previous studies (e.g. [3, 13, 25, 26]). The rates of atrophy observed correspond to within errors with those quoted in the literature. For example, [19] quotes an atrophy rate of $0.05 \pm 0.11\%$ of the brain volume per year in a group of 5 males and 6 females with a mean age of 51.3 years: the current study gives a value of 0.11% at the same age. [18] quotes $0.41 \pm 0.47\%$ in a group of 9 males and 9 females with a mean age of 65.0: the current study gives a value of 0.14% . [6] quotes $0.47 \pm 0.40\%$ per year in a group of 27 subjects with a mean age of 59.6: the current study gives a value of 0.12% [10] $0.41 \pm 0.22\%$ per year in a group of 10 males and 13 females with a mean age of 48 years: the current study gives a value of 0.10% . There is broad agreement in the literature that elevated rates of whole brain atrophy are seen in disease. For example, [19] quotes an atrophy rate of 1.0% of the brain volume per year in a group of 11 Alzheimer’s disease patients with a mean age of 53.8, [10] quotes an atrophy rate of $2.17 \pm 0.52\%$ of the brain volume per year in a group of 8 Alzheimer’s disease patients with a mean age of 54.0, and [6] quotes atrophy rates of 2.37% per year in a group of 54 Alzheimer’s disease patients with a mean age of 61.3 and 3.15% per year in a group of 30 frontotemporal dementia patients with a mean age of 59.3. A more complete survey of such results is given in [18].

Having found a plausible functional fit to the TIV normalised CSF, this function can be used to normalise for age related atrophy in studies where this is a confounding variable, for example when the amount of atrophy due to a neurodegenerative disease is to be quantified. TIV normalised CSF volume measurements can be multiplied by the ratio of the function at the subject’s age to the function at some standard age to normalise age-related atrophy to the amount expected at the standard age. The formulae required are given in the next section. This procedure was adopted here to remove the functional dependence on age from the CSF volume measurements, allowing calculation of the standard deviation of the data (2.29% in terms of the TIV). The standard deviation of the TIV normalised CSF volume measurements within each of the sets of scans for subjects who were imaged multiple times was then calculated: the mean was 0.32% . The standard deviation of the data was therefore 7.3 times larger than this, indicating that the majority of the variability in the data is due to the inherent biological variability of CSF volumes in normal subjects.

3.3 Regional Distribution of CSF Volume Change

In order to investigate the regional distribution of the volume loss, the CSF space was divided into twelve equi-sized boxes as described above. Weibull CDFs were then fitted to the TIV normalised CSF volumes in each box, and to the combinations of the anterior, central and posterior four boxes, and each of the lateral and superior and inferior six boxes, as shown in Fig.9. On inspecting the plots, it appears that the variation can be explained by a single function scaled according to the size of the box i.e. the proportion of the CSF under analysis.

In order to investigate this hypothesis, the fit function was modified slightly. Of the parameters, “a” sets the

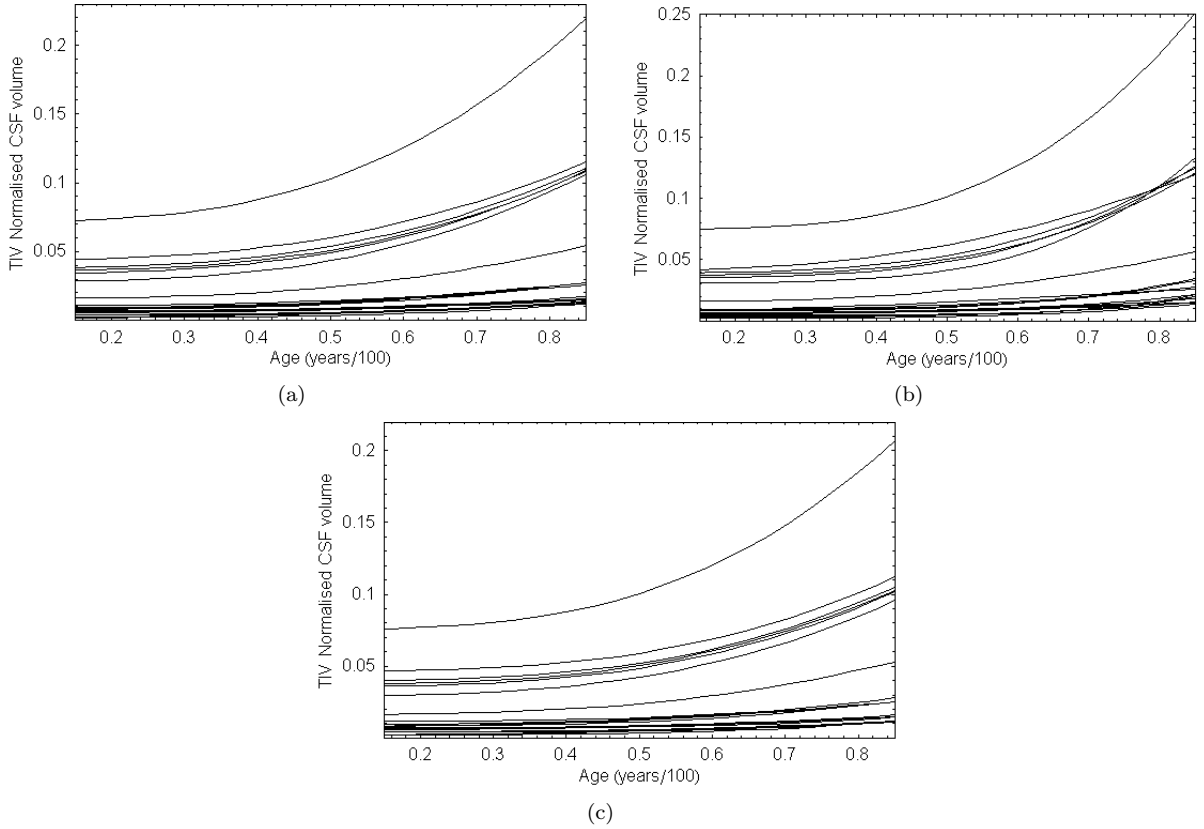


Figure 9: Weibull CDF fits to the TIV normalised CSF volumes in all regions and combinations of contiguous sub-regions for both male and female subjects (a) and male (b) and female (c) subjects separately.

intercept of the function, “b” is a scaling variable on the abscissa, and “c” is the shape parameter. However, we required an overall multiplicative scale parameter (i.e. a scaling parameter on the ordinate), to account for sub-volumes containing less than 100% of the total TIV. Therefore, parameter “b” was fixed to the value determined from the fit to the whole CSF volume, and a multiplicative scale parameter “d” was applied to the function. The fits were repeated, and the parameters plotted against a measure of the amount of the CSF in the box. Ideally this would have been determined from an independent normal brain atlas: however, since the subject group used in this study was large, it was deemed acceptable to use an average of all subjects instead. Therefore, the parameters of the fits were plotted against the the percentage x of the total CSF volume in each region² and are shown in Fig.10. The fits are dependent only on the scale parameter d , which is directly proportional to x (where d/x is the ratio of total CSF volume to TIV, averaged over all subjects). In the modified function, parameter “a” is the scaled intercept of the fit to the total volume. The shape parameter “c” is constant to within errors, proving that for volumes of this size there is no regional dependence of age-related atrophy. Therefore, normalisation factors for age-related atrophy in arbitrary volumes can be interpolated using The parameters given in Table 3 and the function

$$CSF \text{ volume}/TIV = d[a + (1 - a)(1 - e^{-[\frac{age \text{ (years)}]{100b}]^c})]$$

Group	Parameter a	Parameter b	Parameter c	Parameter d	Parameter f	Parameter g
Males	0.0767	1.2893	3.8204	$10.276 \times 10^{-3}x$	0.893	1.580
Females	0.0744	1.5138	3.2831	$9.918 \times 10^{-3}x$	1.035	1.386
All	0.0727	1.4970	3.0885	$9.872 \times 10^{-3}x$	1.355	2.230

Table 3: Parameters of the scaled Weibull CDF, where x is the percentage of the CSF in the volume under analysis. Parameters a, b, c, and d are those of the fits themselves: parameters f and g allow calculation of the RMS errors on the fits.

²This quantity was found to be independent of age at the 95% confidence level, as can be inferred from Fig.4.

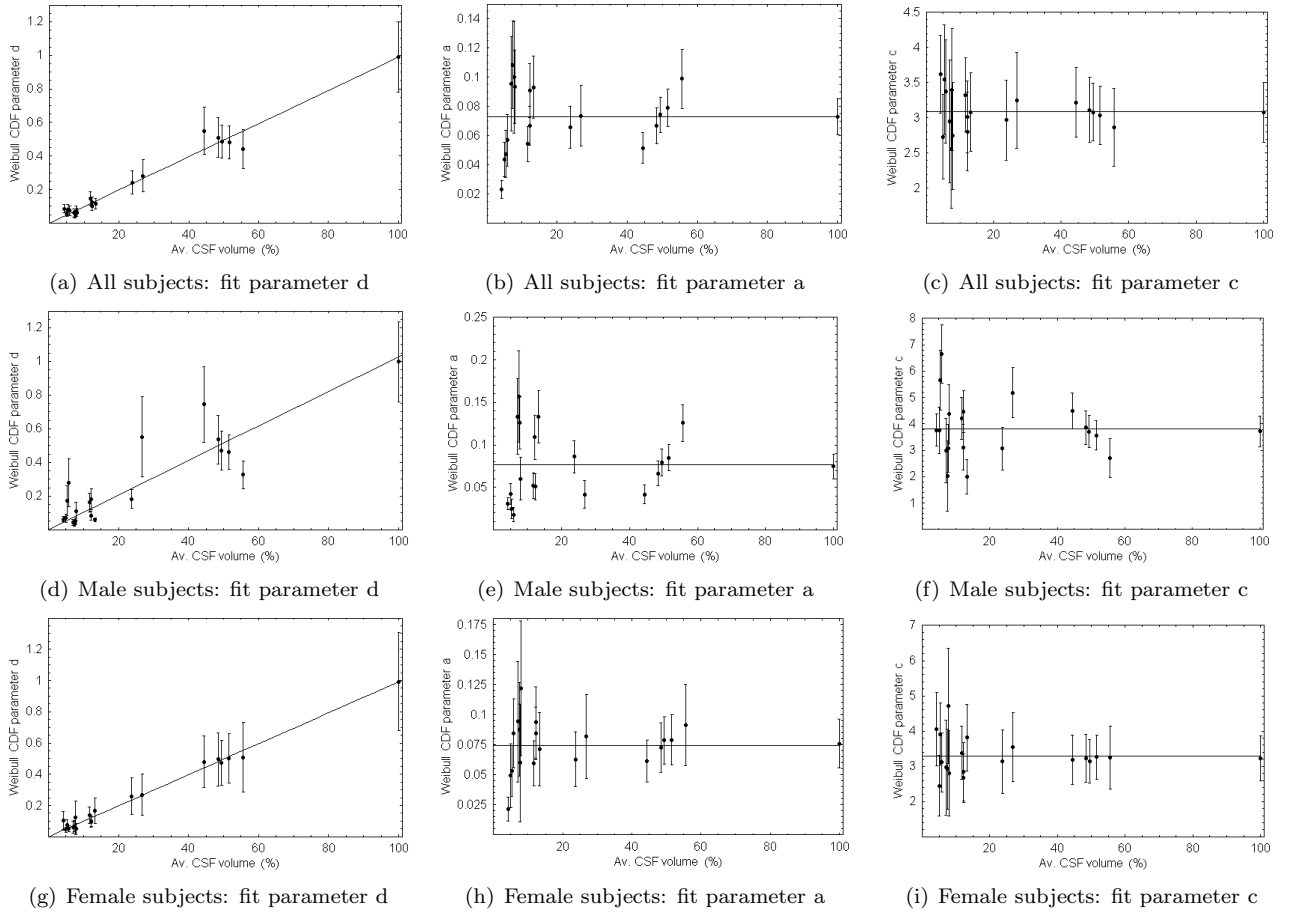


Figure 10: The Weibull fit parameters d , a , and c for all volumes and sub-volumes in all subjects (a, b, c), and male (d, e, f) and female (g, h, i) subjects separately. Errors were estimated from the confidence interval on the fits themselves, and so are correlated across the parameters.

The RMS errors on both interpolated and fitted Weibull CDF functions for all volumes and sub-volumes are shown in Fig. 11. The errors are expected, due to the scaling relationship described above, to have a linear dependence on the percentage of CSF in the region, and linear fits to the data are shown. The increase in RMS errors, averaged across fits to all volumes, for the interpolated functions compared to the functions fitted directly to the data were 5.06% for males, 0.583% for females, and 0.542% for both groups combined. The additional error introduced into any normalisation using the above formula through interpolation, rather than fitting directly to the data, is therefore negligible. The RMS errors obey the dependence

$$RMS \text{ error} = f \times 10^{-3} + g \times 10^{-4}x$$

where the parameters f and g are given in Table 3.

There is a significant body of literature on regional variations in the rate of age related atrophy. For example, [14] observed faster atrophy in frontal lobes than in temporal lobes in both males and females, and faster atrophy in males than females in both regions. However, [6] found no significant regional difference in rates of cerebral atrophy in normal subjects when the brain was divided into four quadrants, and no regional differences in CSF volume change were observed in the current study in twelve regions. It is therefore probable that regional differences in age-related atrophy occur at too small a scale to be observed at the coarse scales studied here. It is also possible that the various structures supporting the brain (the brainstem, optic nerves, falx cerebri, tentorium cerebelli etc.) have some centring effect that acts to hold the brain steady within the cranium, and so regional differences in atrophy rates in grey and white matter will not be observed as regional differences in CSF volume change.

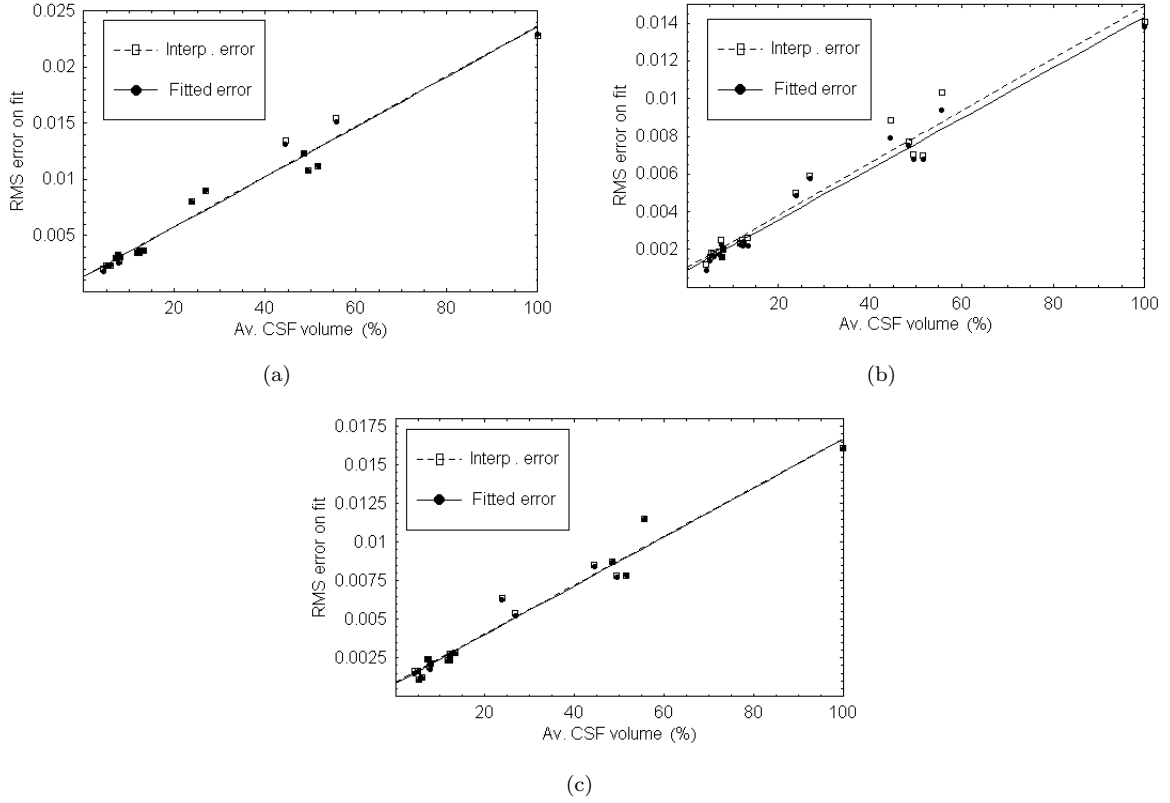


Figure 11: RMS error on fitted and interpolated Weibull CDFs for all sub-volumes for both male and female subjects (a), and male (b) and female (c) subjects separately.

3.4 A Meta-study of TIV-Normalised CSF Volume Measurements

In order to compare the results presented here to those from previous work, a meta-study was performed. Eight papers published between 1991 and 2002, which quoted TIV and CSF volume measurements from MR images in normal subjects, were used. These previous studies used a variety of MR pulse sequences, definitions of the measurement space, and segmentation routines, summarised in Table 4. Therefore, exact agreement between the various data should not be expected: instead, the results are expected to lie on a set of approximately parallel curves, indicating the variation in the volume measurement introduced by the various experimental procedures.

Reference	No. subjects	Definition of measurement space	Segmentation
Gur et. al. 1991 [26]	69 T	Excludes cerebellum	T2/PD 2D histogram fitting
Blatter et. al. 1995 [3]	89 M 105 F	TIV	ANALYZE [38, 11]
Mueller et. al. 1998 [31]	46 T	Excludes brainstem	REGION [28]
Coffey et. al. 1999 [12]	122 M 198 F	Excludes slices below midbrain	MedVision
Chan et. al. 2001 [7]	10 T	TIV	MIDAS [21]
Whitwell et. al. 2001 [44]	55 T	Excludes slices below cerebellum	MIDAS [21]
Good. et. al. 2001 [25]	265 M 200 F	TIV	SPM99 [1]
Chard et. al. 2002 [9]	13 M 14 F	Excludes slices containing cerebellum	SPM99 [1]

Table 4: Details of the experimental method adopted by studies used in the meta-study, showing the number of subjects included (M=male; F=female; T=total, where the number of each sex was not given), the definition of the measurement space (where TIV is indicated, the whole CSF pool inside the cranium was used), and the software used to perform the segmentation.

Scattergrams of the meta-study data are given in Fig.12 for volumes averaged across both sexes (a), and for males (b) and females (c) separately. Plots of the Weibull CDF fits to the data presented here (i.e. not of fits to the data

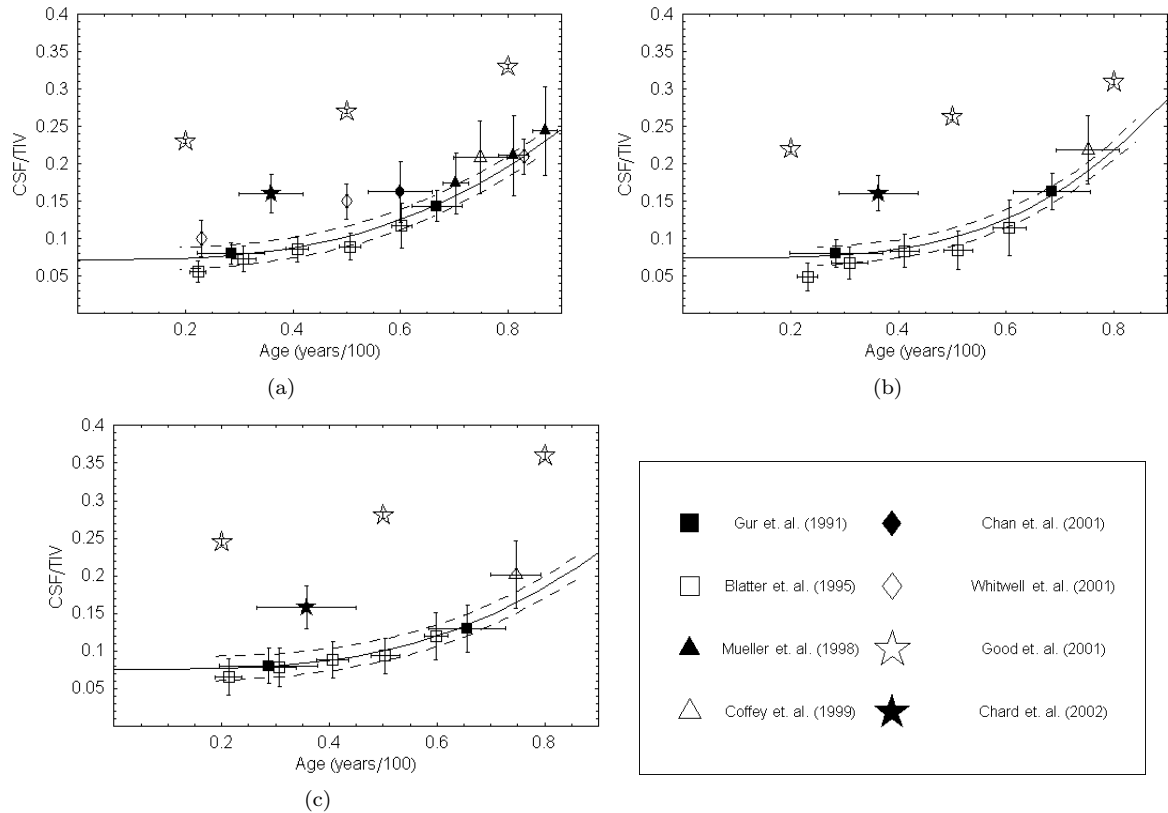


Figure 12: Previous published TIV normalised CSF volume measurements for the average of both sexes (a), males (b) and females (c). The solid curves show Weibull fits to the data presented in this paper: the dashed curves are the upper and lower 1σ error bounds. The points show data from the literature. Points with error bars in both the x and y directions represent data published numerically, whilst points with error bars only in the y direction represent data read from graphs.

shown in the graphs), are also shown in each case. Most of the data show a remarkable level of consistency with each other and with the Weibull CDF curves, considering the variations in the experimental procedures. Indirectly, this implies that across these studies as a whole, the variations in volume measurements introduced by the different experimental procedures are comparable to or smaller than the inherent biological variability in total intracranial and CSF volumes. Some outliers are present, representing the results published in [25] and [9], both of which used SPM'99 to perform the segmentation. Significantly higher CSF volumes were quoted by these authors than are supported by the rest of the literature. However, the magnitude of the disagreement with the rest of the literature, particularly in the case of [25], is too great to explain as genuine measurements of unexpectedly high CSF volumes. It seems more plausible that these results represent methodological flaws in the studies concerned. Therefore we conclude that the CSF volume measurements presented here are in good agreement with the literature, and that the hypothesised Weibull CDF model of TIV-normalised CSF volume is sufficient to explain all of the statistically significant functional dependence of that quantity on age.

4 Conclusion

In previous work [42] we have shown the feasibility of developing fully automatic diagnostic systems for neurodegenerative diseases using regional measurements of CSF volume as a surrogate for measuring cerebral atrophy. Normalisation for the major confounding effect of age-related atrophy is required in order to identify the influence of disease on such measurements. This paper has presented such a normalisation. It has shown that age-related atrophy occurs significantly faster in males than in females, but can plausibly be described by a Weibull CDF in both sexes, and that the atrophy occurs evenly throughout the brain at the scale of arbitrary ($\approx 10 - 100cm^3$) volumes. Therefore, interpolated correction factors can be produced for any region based on the proportion of the CSF located in that region, determined from a normal brain atlas. However, this simple relationship may fail for small volumes containing specific structures, particularly in the brain stem.

Cerebral volume measurements also frequently require normalisation for head size or variations in voxel dimensions, often achieved by normalising to TIV. This paper has shown that normalisations to the volume of the bounding box on the CSF space and to TIV are statistically equivalent, to within the limitations imposed by segmentation errors. Therefore, in studies that involve analysis of CSF distribution, this equivalence removes the need to measure TIV, avoiding a potential source of error and reducing the computational overhead. No indication of a statistically significant dependence of TIV on age was found, but males were found to have a significantly higher average TIV than females. The calculation of the bounding box volume takes into account the first three modes of variation of the TIV i.e. the anterior-posterior, lateral, and superior-inferior dimensions. The results therefore demonstrate that the TIV is dominated by these first three modes of variation i.e. more detailed inter-subject variations in the shape of the cranium are small compared to the segmentation errors in this study. Males were found on average to have a significantly (8%, $P < 0.01$) higher TIV than females.

Identification of the functional behaviour of age-related atrophy as a Weibull CDF allows speculation on the underlying biological processes. It indicates that the atrophy is due to the loss of discrete (presumably cellular) units within the brain, with a time-dependent (power law) probability of decay. Such behaviour is observed in systems where the decay of a given unit increases the probability of decay in those remaining: this is an entirely plausible mechanism in a highly interlinked system such as the brain.

Acknowledgements

We would like to acknowledge the assistance of Prof. Alastair Burns and Prof. Charles McCollum in gathering the data used in this study. This work was funded by the MIAS (Medical Images and Signals) IRC under EPSRC grant no. GR/N14248/01 and the UK Medical Research Council Grant No. D2025/31, and by the Wellcome Trust grant no. ME003889. The software used in this study is freely available from www.tina-vision.net.

References

- [1] J Ashburner and K Friston. Multimodal image coregistration and partitioning—a unified framework. *NeuroImage*, 6:209–217, 1997.
- [2] R Barber, C Ballard, I G McKeith, A Gholkar, and J T O’Brien. Mri volumetric study of dementia with lewy bodies: a comparison with ad and vascular dementia. *Neurology*, 54:1304–1309, 2000.
- [3] D D Blatter, E D Bigler, S D Gale, S C Johnson, C V Anderson, B M Burnett, N Parker, S Kurth, and S D Horn. Quantitative volumetric analysis of brain mr: Normative database spanning 5 decades of life. *American Journal of Neuroradiology*, 16:241–251, 1995.
- [4] P A Bromiley, M Pokric, and N A Thacker. Computing covariances for mutual information coregistration. In *Proceedings MIUA ’04*, pages 77–80, 2004.
- [5] P A Bromiley, M Pokric, and N A Thacker. Empirical evaluation of covariance estimates for mutual information coregistration. In *Proceedings MICCAI’04*, pages 607–614, 2004.
- [6] D Chan, N C Fox, R Jenkins, R I Scahill, W R Crum, and M N Rossor. Rates of global and regional cerebral atrophy in ad and frontotemporal dementia. *Neurology*, 57:1756–1763, 2001.
- [7] D Chan, N C Fox, R I Scahill, W R Crum, J L Whitwell, G Leschziner, A M Rossor, J M Stevens, L Cipolotti, and M N Rossor. Patterns of temporal lobe atrophy in alzheimer’s disease. *Annals of Neurology*, 49:433–442, 2001.
- [8] D T Chard, C M Griffin, G J M Parker, R Kapoor, A J Thompson, and D H Miller. Brain atrophy in clinically early relapsing-remitting multiple sclerosis. *Brain*, 125:327–337, 2002.
- [9] D T Chard, G J M Parker, C M B Griffin, A J Thompson, and D H Miller. The reproducibility and sensitivity of brain tissue volume measurements derived from an spm-based segmentation methodology. *JMRI*, 15:259–267, 2002.
- [10] K Chen, E M Reiman, G E Alexander, D Bandy, R Renaut, W R Crum, N C Fox, and M N Rossor. An automated algorithm for the computation of brain volume change from sequential mris using an iterative principle component analysis and its evaluation for the assessment of whole-brain atrophy rates in patients with probable alzheimer’s disease. *NeuroImage*, 22:134–143, 2004.
- [11] H E Cline, W E Lorensen, R Kinikis, and F Jolesz. Three-dimensional segmentation of mr images of the head using probability and connectivity. *Journal of Computer Assisted Tomography*, 14:1037–1045, 1990.
- [12] C E Coffey, J A Saxton, G Ratcliff, R N Bryan, and J F Lucke. Relation of education to brain size in normal aging: Implications for the reverse hypothesis. *Neurology*, 53:189–196, 1999.
- [13] E Courchesne, H J Chisum, J Townsend, A Cowles, J Covington, B Egaas, M Harwood, S Hinds, and G A Press. Normal brain development and aging. *Neuroradiology*, 216:672–682, 2000.

- [14] P E Cowell, B I Turetsky, R C Gur, R I Grossman, D L Shtasel, and R E Gur. Sex differences in aging of the human frontal and temporal lobes. *Neuroscience*, 14:4748–4755, 1994.
- [15] A T Du, N Schuff, D Amend, M P Laakso, Y Y Hsu, W J Jagust, K Yaffe, J H Kramer, B Reed, D Norman, H C Chui, and M W Weiner. Magnetic resonance imaging of the entorhinal cortex and hippocampus in mild cognitive impairment and alzheimer’s disease. *J Neurol Neurosurg Psychiatry*, 71:441–447, 2001.
- [16] C Enzinger, F Fazekas, P M Matthews, S Ropele, H Schmidt and S Smith, and R Schmidt. Risk factors for progression of brain atrophy in aging. six year follow up of normal subjects. *Neurology*, 64:1704–1711, 2005.
- [17] M F Folstein, S E Folstein, and P R McHugh. ”mini-mental state”. a practical method for grading the cognitive state of patients for the clinician. *J Psychiatr Res*, 12:189–198, 1975.
- [18] N C Fox, S Cousens, R Schill, R J Harvey, and M N Rossor. Using serial registered brain magnetic resonance imaging to measure disease progression in alzheimer disease. *Archives of Neurology*, 57:339–344, 2000.
- [19] N C Fox, P A Freeborough, and M N Rossor. Visualisation and quantification of rates of atrophy in alzheimer’s disease. *The Lancet*, 348:94–97, 1996.
- [20] N C Fox and J M Schott. Imaging cerebral atrophy: normal ageing to alzheimer’s disease. *Lancet*, 363:392–394, 2004.
- [21] P A Freeborough, N C Fox, and R I Kitney. Interactive algorithms for the segmentation and quantitation of 3-d mri brain scans. *Comput. Methods Prog. Biomed*, 53:15–25, 1997.
- [22] G B Frisoni, P Scheltens, S Galluzzi, F M Nobili, N C Fox, P H Robert, H Soininen, L O Wahlund, G Waldemar, and E Salmon. Neuroimaging tools to rate regional atrophy, subcortical cerebrovascular disease, and regional cerebral blood flow and metabolism: consensus paper of the eadc. *J Neurol Neurosurg Psychiatry*, 74:1371–1381, 2003.
- [23] C J Galton, B Gomez-Anson, N Antoun, P Scheltens, K Patterson, M Graves, B J Sahakian, and J R Hodges. Temporal lobe rating scale: application to alzheimer’s disease and frontotemporal dementia. *J Neurol Neurosurg Psychiatry*, 70:165–173, 2001.
- [24] Y Ge, R I Grossman, J S Babb, M L Rabin, L J Mannon, and D L Kolson. Age-related total gray matter and white matter changes in normal adult brain. part i: Volumetric mr imaging analysis. *Am J Neuroradiol*, 23:1327–1333, 2002.
- [25] C D Good, I S Johnsrude, J Ashburner, R N A Henson, K J Friston, and R S J Frackowiak. A voxel-based morphometric study of ageing in 465 normal adult human brains. *NeuroImage*, 14:21–36, 2001.
- [26] R C Gur, P D Mozley, S M Resnick, G L Gottlieb, M Kohn, R Zimmerman, G Herman, S Atlas, R Grossman, D Berretta, R Erwin, and R E Gur. Gender differences in age effect on brain atrophy measured by magnetic resonance imaging. *Proc. Natl. Acad. Sci. USA*, 88:2845–2849, 1991.
- [27] R Jenkins, N C Fox, A M Rossor, A J Harvey, and M N Rossor. Intracranial volume and alzheimer disease: Evidence against the cerebral reverse hypothesis. *Archives of Neurology*, 57:220–224, 2000.
- [28] J A Kaye, T Swihart, D B Howieson, A Dame, M M Moore, T Karnos, R M Camicioli, M Ball, B Oken, and G Sexton. Volume loss of the hippocampus and temporal lobe in healthy elderly persons destined to develop dementia. *Neurology*, 48:1297–1304, 1997.
- [29] R J Killiany, T Gomez-Isla, M Moss, R Kikinis, T Sandor, F Jolesz, R Tanzi, K Jones, B T Hyman, and M S Albert. Use of structural magnetic resonance imaging to predict who will get alzheimer’s disease. *Ann. Neurol.*, 47:430–439, 2000.
- [30] D S Knopman, S T DeKosky, J L Cummings, H Chui, J Corey-Bloom, N Relkin, G W Small, B Miller, and J C Stevens. Practice parameter: diagnosis of dementia (an evidence-based review). report of the quality standards subcommittee of the american academy of neurology. *Neurology*, 56:1142–1153, 2001.
- [31] E Mueller, M M Moore, D C R Kerr, G Sexton, R M Camicioli, D B Howieson, J F Quinn, and J A Kaye. Brain volume preserved in healthy elderly through the eleventh decade. *Neurology*, 51:1555–1562, 1998.
- [32] N Purandare N, C Ballard, and A Burns. Preventing dementia. *Advances in Psychiatric Treatment*, 11:176–187, 2005.
- [33] R C Petersen, R Doody, A Kurz, R C Mohs, J C Morris, P V Rabins, K Ritchie, M Rossor, L Thal, and B Winblad. Current concepts in mild cognitive impairment. *Arch Neurol*, 58:1985–1992, 2001.
- [34] M Pokrić, N A Thacker, and A Jackson. The importance of partial voluming in multi-dimensional medical image segmentation. In *Proc. MICCAI*, pages 1293–1294, 2001.
- [35] M Pokrić, N A Thacker, M L J Scott, and A Jackson. Multi-dimensional medical image segmentation with partial voluming. In *Proc. MIUA*, pages 77–80, 2001.
- [36] W H Press, B P Flannery, S A Teukolsky, and W T Vetterling. *Numerical Recipes in C*. Cambridge University Press, New York, 2nd edition, 1992.
- [37] S M Resnick, D L Pham, M A Kraut, A B Zonderman, and C Davatzikos. Longitudinal magnetic resonance imaging studies of older adults: A shrinking brain. *J Neurosci.*, 23:3295–3301, 2003.
- [38] R A Robb. A software system for interactive and quantitative analysis for biomedical images. In K H Hohne, H Fuchs, and D M Pizer, editors, *3D imaging in medicine*, volume F60, pages 333–361. NATO ASI Series, 1990.
- [39] R I Schill, C Frost, R Jenkins, J L Whitwell, M N Rossor, and N C Fox. A longitudinal study of brain volume changes in normal aging using registered magnetic resonance imaging. *Arch. Neurol.*, 60:989–994, 2003.

- [40] N A Thacker and P A Bromiley. Tina memo 2001-010: The effects of a square root transform on a poisson distributed quantity. Technical report, Imaging Science and Biomedical Engineering Division, University of Manchester, 2001.
- [41] N A Thacker, M Pokrić, and D C Williamson. Noise filtering and testing illustrated using a multi-dimensional partial volume model of mr data. In *Proc. BMVC*, pages 909–919, Kingston, London, 2004.
- [42] N A Thacker, A R Varma, D Bathgate, S Stivaros, J S Snowden, D Neary, and A Jackson. Dementing disorders: Volumetric measurement of cerebrospinal fluid to distinguish normal from pathological findings; feasibility study. *Radiology*, 224(1):278–285, 2002.
- [43] W Weibull. A statistical theory of the strength of materials. In *The Royal Swedish Inst. Eng. Proc. No. 151*, 1939.
- [44] J L Whitwell, W R Crum, H C Watt, and N C Fox. Normalisation of cerebral volumes by use of intracranial volume: Implications for longitudinal quantitative mr imaging. *American Journal of Neuroradiology*, 22:1483–1489, 2001.